Accepted Manuscript

Interactions between nanoparticles in nanosuspension

N. Kovalchuk, D. Johnson, V. Sobolev, N. Hilal, V. Starov

PII: S0001-8686(19)30194-0
DOI: https://doi.org/10.1016/j.cis.2019.102020
Article Number: 102020
Reference: CIS 102020

To appear in: *Advances in Colloid and Interface Science*

Received date: 28 May 2019
Revised date: 9 August 2019
Accepted date: 14 August 2019

Please cite this article as: N. Kovalchuk, D. Johnson, V. Sobolev, et al., Interactions between nanoparticles in nanosuspension, Advances in Colloid and Interface Science, https://doi.org/10.1016/j.cis.2019.102020

Interactions between nanoparticles in nanosuspension

N. Kovalchuk[1], D. Johnson[2], V. Sobolev[3], N. Hilal[2,4], V. Starov[5]

[1] University of Birmingham, UK

[2] Swansea University, UK

[3] A.N.Frumkin Institute of Physical Chemistry and Electrochemistry , Russian Academy of Sciences, Russia

[4] NYUAD Water Research Centre, New York University Abdu Dhabi, Abu Dhabi, United Arab Emirates

[5] Loughborough University, UK

Abstract

Nanoparticles are particles with a characteristic dimension below 100 nm. The properties of nanoparticles differ substantially from those of “big” colloidal particles (size bigger than 1 μm) because radius of surface forces, which is around 100 nm, is greater than or comparable with the nanoparticles size. The latter means that each nanoparticle could be completely covered by the surface forces of the neighbouring particles at small enough separation. It also means that the well-known Derjaguin approximation cannot be applied directly and some modifications are required. Pairwise interaction between nanoparticles can be used only at an extremely low volume fraction of nanoparticles (below some critical volume fraction, which is ~0.02%), and above this concentration a new theory based on many-particle interactions should be applied, which is yet to be developed. Some recent progress in the area of interaction between nanoparticles is reviewed and the properties of nanosuspensions based on interaction between nanoparticles are described. The authors have not attempted to cover all available literature in the area but instead have tried to underline the fundamental problems in the area which need to be addressed.

1. Introduction

Nanoparticles are particles typically characterised by having a radius, or rather a characteristic size, below 100 nm. From one side nanoparticles fall into the category of regular colloidal objects because their interactions with other particles and between nanoparticles are of a well-known colloidal nature [1]: London–van der Waals forces, electrical double layer forces, solvation forces, hydrophobic forces and

steric forces. That is, nanoparticles and their interactions are in the framework of Derjaguin–Landau–Verwey–Overbeek (DLVO) theory [2]. All these forces are referred below as “surface forces”. It is important to emphasise that the radius of action of surface forces is around 100 nm. That is, two regular colloidal particles (characteristic size around 1 μm) or nanoparticles (characteristic size less than 100 nm) start interacting if the shortest distance between them is less than the radius of surface forces action, that is, 100 nm.

The latter determines a very special feature of nanoparticles, which makes them differ from regular colloidal particles: the size of regular colloidal particles is larger than the radius of surface forces action, while the size of nanoparticles is smaller. This difference results in in a very substantial difference in the interaction of nanoparticles as compared with regular colloidal particles.

To understand the difference between interactions of particles of different sizes let us consider a simple model of colloidal or nano-colloidal suspension: a cubic model (Fig. 1).

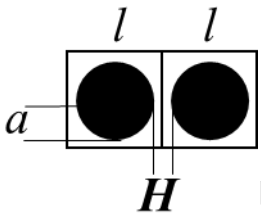

Fig. 1. Cell model: the volume per particle is ℓ^3. *a* is the radius of a particle, *H* is the closest distance between particles: $\ell = 2a + H$

The particle volume fraction, φ, according to Fig. 1 can be presented as $\varphi = (4\pi/3)a^3/\ell^3 = (4\pi/3)a^3/(2a + H)^3 = (\pi/6)(1/(1 + H/2a)^3)$, where $\pi/6$~0.52 is the close packing volume fraction in the cubic cell model. The range of surface forces is *Hs~100* nm [1]. Let us define a critical volume fraction of particles, φ_{cr}, such that the distance between particles, *H,* equals H_s*~100* nm, i.e., $\varphi_{cr} = (\pi/6)(1/(1 + H_s/2a)^3)$. This means that the particle at volume fraction $\varphi < \varphi_{cr}$ do not interact and the suspension may be considered to be dilute (Fig. 2). However, for $\varphi > \varphi_{cr}$ the particles strongly interact and form an interconnected network and at such concentration suspensions can be referred to as concentrated (Fig. 3a and b).

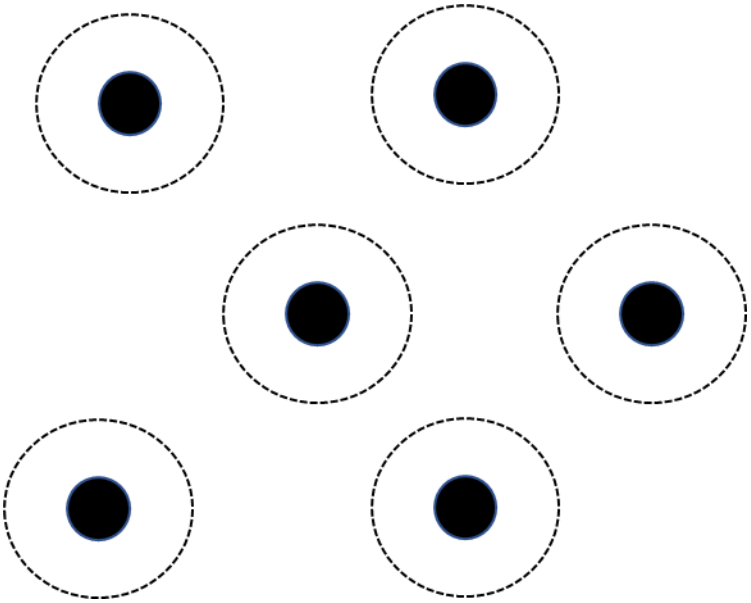

Fig. 2. Diluted suspension/nanosuspension at $\varphi < \varphi_{cr}$: average distance between particles/nanoparticles is larger than the radius of surface forces action. Particles are in black, circles are radius of surface forces action.

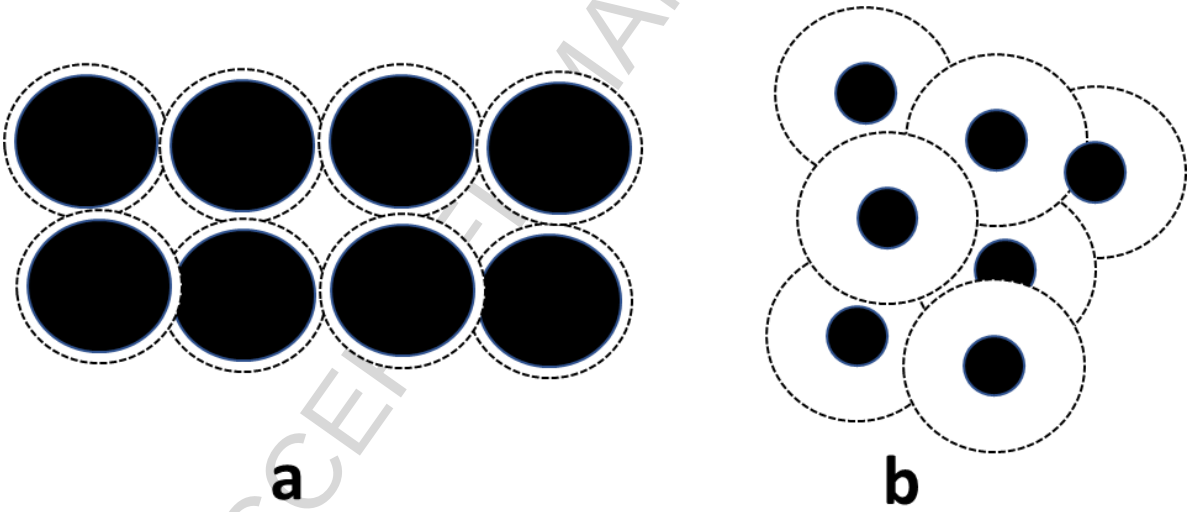

Fig. 3. Concentrated suspension of colloidal particles at $\varphi > \varphi_{cr}$: a –radius of surface forces action is smaller than the particles radius (regular colloidal suspension); b – radius of surface forces is bigger than the particle radius (nanosuspension).

Such concentrated suspensions have very different properties from those of dilute suspensions. For regular colloidal suspensions *a*~1 μm and φ_{cr}~0.45 (Fig. 3a), i.e., a value near to the close packing volume fraction. However, for nanoparticles *a*~10 nm and φ_{cr}~0.02 (Fig. 3b), suspensions at such low volume fractions are usually considered to be very dilute, in stark contrast to the case of nano-suspensions. Even

at such a low volume fraction, φ, the particles strongly interact, making all properties of such a nano-suspension unavoidably different from those of a normal dilute suspension.

The latter means that the viscosity of nano-suspensions will be considerably larger than the viscosity of the dispersion medium, even at such low volume concentrations as 0.01,which has been confirmed by numerous experimental results [3, 4]. It is notable that the classical viscosity models do not work for nano-suspensions and so far there is no model or correlation capable of precise prediction of the viscosity of nano-suspensions with respect to their volume fractions [3, 4]. Moreover, suspensions formed by carbon nano-tubes demonstrate transition to non-Newtonian behaviour at very low solid volume fractions, sometimes even below 1 % [5].

These observations prove that the behaviour of nano-suspensions is very much different from that of regular colloidal suspensions. Below we try to explain this difference, which is based on colloidal interactions between nanoparticles.

Figs. 3a and 3b demonstrate an additional feature in colloidal interaction between regular colloidal particles and nanoparticles. In the case of regular colloidal particles (Fig. 3a) ranges of surface forces action from neighbouring particles overlaps only in a narrow vicinity of the shortest distance between particles. In this case Derjaguin's approximation can be used [6]. Derjaguin's approximation means that the interaction is integrated over a narrow region close to the shortest distance between interacting particles.

However, Fig. 3b shows that Derjaguin's approximation cannot be used in the case of nanoparticles. Figs. 3a and 3b also demonstrate an additional very substantial difference of nano-particle interactions from that of regular colloidal particles. According to Fig. 3a the interaction between two neighbouring colloidal particles is pairwise interaction. However, Fig. 3b shows that the ranges of interaction of many nanoparticles overlap. The latter means that interactions between nanoparticles at concentrations above a very low critical concentration are not pairwise but collective in nature and can therefore be non-additive [7]. To the best of our knowledge the collective interaction of nanoparticles in nano-suspensions at concentrations above critical has never been investigated.

The next special feature of nanoparticles is their much larger diffusion coefficient, *D*, compared to regular colloidal size particles, which is inversely proportional to the

radius of particles *a*: $D = \frac{kT}{6\pi\eta a}$, where *kT* is the thermal energy of fluctuations and η is dynamic viscosity of the surrounding fluid. Hence, the ratio of the diffusion coefficient of a nano-particle (10 nm) and a regular colloidal particle (a~ 1 μm) is equal to 100. That is, diffusion of nanoparticles is much faster as compared with regular colloidal particles.

Summarizing the above, nanoparticle interactions and behaviour of nano-suspensions is different from suspensions of regular colloidal particles because of the following four reasons:

1. Range of interactions between nanoparticles is larger than the nano-particle's radius. To the best of our knowledge, there is no complete theory for these interactions.
2. As a result of a large radius of interaction relative to the particle size, the critical volume concentration of nano-suspensions (the concentration when all particles are interconnected) is very low in comparison with colloidal suspension of micron size particles.
3. At concentrations above critical the interaction between nanoparticles cannot be treated as pairwise but becomes collective. To the best of the author's knowledge, there has not been a single attempt reported to take this into account.
4. Diffusion coefficient of nanoparticles is substantially greater than the corresponding coefficient of regular colloidal particles.

2. Theory of colloidal interactions

Modern physical theory, which quantitatively describes the state and stability of dispersed systems, is based on calculations and analysis of surface forces acting in layers of liquids between interacting particles [6]. Surface forces play a role in colloid science, such as the forces of intermolecular interactions in condensed bodies.

Surface forces determine the equilibrium distances between the particles of dispersions, as well as the conditions of their coagulation, the number and strength of the bonds formed between the particles. The physical nature of surface forces is different for different components. Their most investigated component is the dispersion forces caused by overlapping of fluctuations of electromagnetic fields acting through a layer separating the particle surfaces. In the case of charged

particle surfaces, electrostatic forces also begin to play a significant role. When interacting in aqueous medium hydrophilic or hydrophobic surfaces manifest the effect of structural forces arising from the convergence and overlap of the boundary layers of water with a modified, under the influence of contact with surfaces, structure.

For regular relatively large colloidal particles [1], the theory of surface forces is sufficiently developed and has been applied for many years, providing a fundamental basis for solving many technological problems, such as the management of the state and properties of dispersions, surface wetting, optimization of flotation and water treatment processes, as well as a range of environmental problems. The action of surface forces is the theoretical basis of modern colloid and interface science [6,8].

Calculations of stability and assessment of colloidal dispersions and wetting films of liquids are based on the solutions of the theory of surface forces obtained for the interaction of flat infinitely extended surfaces. Based on this solution with the help of the well-known Derjaguin approximation [6,9] the solution can be extended to the interaction of colloidal particles. Within the framework of this approach, it is possible to calculate the force*, F,* and energy, *U*, of the pairwise interaction of colloidal particles. For two non-planar particles, the force *F* can be determined on the basis of solutions obtained for the interaction energy of two plane surfaces G_{II} (H) [6]:

$$F = C(z)\, G_{II}(H), \quad (1)$$

where *F* is the interaction force of curved surfaces on the shortest distance, *H*, between them, $G_{II}(H)$ is the energy of interaction between flat surfaces at the same distance and *C(z)* is the geometrical factor of the surfaces, where *z* is the axis of symmetry for the system of interacting particles [6]. For identical spherical particles $C(z) = \pi a$, where a is their radius. For identical cylinders crossed at an angle 90° $C(z) = 2\pi a$.

In [10] a Derjaguin's approximation was applied to the case of interaction between a charged particle and a pore in a charged membrane surface, that is, a method to calculate interaction energy between convex and concave surfaces.

However, Derjaguin's approximation has a limited range of applicability, since it can be used only for particles with radii $a>0.1\ \mu m$, where *0.1 μm* is the characteristic scale of surface forces action. This determines, in fact, the lower boundary of the colloidal particle size, for which it is still possible to use the equations of the DLVO

theory [6], obtained for the interaction of flat surfaces. This defines the boundary between the large regular colloidal particle with a radius of more than *0.1 μm* and smaller particles, which can be referred to as nanoparticles, for which other solutions must be obtained. The boundary between large colloidal particles and nanoparticles is largely conditional and is determined only by differences in methods for calculating the interaction forces between particles.

It is easy to show that for colloidal particles, when Eq. (1) is applicable, the energy of their pair interaction (dispersion, electrostatic and structural) is linearly dependent on the particle radius, without detecting deviations from this pattern with a decrease in their sizes down to *0.1 μm* [8], if it was assumed that the material properties of the particles do not change with size.

In the case of nanoparticles, the approximation of Eq. (1), due to the large curvature of the surface of small particles, can no longer be applied. In this case, other solutions obtained on the basis of direct calculations of the forces and energy of the pair interaction of nanoparticles should be found.

It is important to emphasise that the consideration below is valid for dilute suspension of nanoparticles, when the concentration of nanoparticles is below the critical one and the interaction can be considered as pairwise one.

One of the first solutions of the problem of electrostatic interaction of small particles was obtained by Derjaguin [11] for the case of strong overlapping of electrical double layers (EDS), when the shortest distance between the surfaces of particles, *H,* was much smaller than their radius *a*. The energy of electrostatic interactions of two small particles at a low electrolyte concentration in the dispersion medium surrounding them was obtained as [11]:

$$U_e(H) = \frac{\varepsilon_0 \varepsilon_r a^2 \psi^2}{2a+H}, \qquad (2)$$

where ε_0 and ε_r are the permittivity of vacuum and relative permittivity of the medium respectively, *a* is the radius of the particles and ψ is the electric potential of their surfaces (zeta potentials).

Later the solution (2) was generalized including the case of small particle surface electric potentials ψ [12]:

$$U_e(H) = \frac{\varepsilon_0 \varepsilon_r a \psi^2 (a+H)}{(2a+H)} ln\left\{1 + \frac{a \exp(-\kappa H)}{(a+H)}\right\}, \quad \text{at } \kappa a > 5, \qquad (3)$$

where $1/\kappa$ is the Debye radius, which depends on the electrolyte concentration.

Unfortunately, both Eqs. (2) and (3) were deduced for the case κa>5 [12], that is for relatively big particles as compared with the thickness of the Debye layer. The latter means that these equations can be applied to nanoparticles at relatively high electrolyte concentrations, when the thickness of the Debye layer is small.

The expression for electrostatic interaction at κa<5 was deduced in [13]:

$$U_e(H) = \frac{4\pi\varepsilon_0\varepsilon_r a^2\psi^2}{(2a+H)}\exp(-\kappa H). \qquad (3a)$$

However, it is necessary to keep in mind that the latter equation gives a relatively low precision of around 40% [13].

The estimations carried out based on Eqs. (3, 3a) showed that the energy of electrostatic repulsion (keeping all other parameters constant) decreases as the particle size decreases, which brings the dispersion of small particles closer to the beginning of coagulation.

It should be taken into account, however, that in the case of nanoparticles, due to the small area of their surface, it is also necessary (or at least possible) to take into account the influence of the discreteness of the distribution of surface charges [14]. According to [14] the discrete charges appear to generate greater interaction potential compared to uniformly charged surfaces. Hence, at the distance between charges, *l*, on the surface *l* > *1/k*, the best approximation for the calculation of electrostatic forces may be the placement of all surface charges in the centre of a small particle.

Analytical model for electrostatic interaction under assumption of non-uniformly distributed surface charge proposed in [15] shows that non-uniformity in charge density can result in electrostatic attraction of similar particles. It was suggested in particular, that hydrophobic attraction may be a result of the charge non-uniformity.

Thus, in the case of nano-dispersions, calculations of electrostatic forces, as can be seen from the above, may differ from well-known solutions for colloidal particles.

We now turn to the consideration of the nature of the dispersion forces of attraction in the nano-dispersions. Both a classical perturbation theory [16] and a direct integration [17] should be modified for calculation of the van-der-Waals (vdW) part of the interaction potential, U_{vdW}, between nanoparticles and a nano-particle with a colloidal probe. In this way a dependency of vdW potential is deduced as a function of all other physical parameters. However, there are reasonable doubts that the Hamaker constant calculated in this way for nanoparticles is correct [18].

Calculations of the attraction forces between nanoparticles on the basis of the macroscopic theory of dispersion forces were carried out after the problem of the attraction forces of nanoparticles was reduced to the interaction of surface plasmons in [19, 20]. The equivalence of this method of calculations with the macroscopic theory of Lifshitz [1] has been previously shown [19, 21]. Based on this method, Mitchell and Ninham [22] obtained the equation for the interaction energy of particles with radius *a* for the case of small thickness of the layer between them, *H*, compared to the radii of the particles. This solution showed that the energy of the dispersion attraction of small particles decreases with a decrease in their size more sharply than in the case of larger, colloidal particles. The solution obtained in [21] for the interaction energy of small particles at small separations contains, in contrast to the known expressions for the big colloidal particles, $U_d(H) = -\frac{Aa}{12\pi H^2}$, where *A* is Hamaker constant, two terms:

$$U_d(H) = -\frac{1}{12}\left[A_1\frac{a}{H} - 2A_2 ln\frac{a}{H}\right], \quad (5)$$

where

$$A_1 = -\frac{3h}{4\pi}\int_0^\infty \Delta_{13}^2 d\xi \quad (6)$$

$$A_2 = -\frac{3h}{4\pi}\int_0^\infty (1-\Delta_{13}^2) ln(1-\Delta_{13}^2) d\xi, \quad (7)$$

where $\Delta_{13} = \frac{\varepsilon_1(\xi)-\varepsilon_3(\xi)}{\varepsilon_1(\xi)+\varepsilon_3(\xi)}$ and ε(ξ) are frequency dependences of the permittivity of the solid phase, ε_1, and the liquid layer, ε_3.

For the calculations of dispersion interaction of nanoparticles in aqueous solutions the following first approximation for calculation of Hamaker constant can be used as suggested in [23] for SiO_2 ($A=4.3 \cdot 10^{-21}$ J), TiO_2 ($A=54.2 \cdot 10^{-21}$ J), Al_2O_3 ($A=33 \cdot 10^{-21}$ J), diamond ($A=13 \cdot 10^{-20}$ J) and other materials. The values of the constant A_1 in Eqs. (5) and (6) is assumed to be equal to the Hamaker constant A. Note, theoretical analysis carried out in [24] has shown that for metallic nano-particles with size smaller than the mean free path of the conducting electrons (~ 50 nm) dielectric permittivity and therefore Hamaker constant becomes size-dependent.

For nanoparticles, the influence of the second term in Eq. (5) should be taken into account. Precise calculations require the use of full spectral data for these calculations. However, in some cases it is possible to use proposed by Krupp [25] empirical expression for the functions $\Delta_{ik}(\xi)$:

$$\Delta_{ik} = \frac{\varepsilon_i(\xi) - \varepsilon_k(\xi)}{\varepsilon_i(\xi) + \varepsilon_k(\xi)} = a_{ik} \exp(-b_{ik}\xi), \quad (8)$$

where a_{ik} and b_{ik} are some constants whose values can be found in [6]. Eq. (8) provides a reasonable approximation for functions $\Delta_{ik}(\xi)$ in the frequency range 10^{16}-10^{17} rad/s, which give the main contribution to the dispersion forces.

The following constants for quartz particles in water were used in the calculations below: $a_{ik}=0.12$ and $b_{ik} = 3.1 \cdot 10^{-17}$ s/rad, obtained in [26]. The use of these constants results in the following value of the Hamaker constant: $A = 1.4 \cdot 10^{-20}$ J, which is used in calculations below.

In Fig. 4 the results of calculations of the dependence of the interaction energy $U(H)= U_d(H) + U_e(H)$ on the shortest distance H between the surfaces of spherical particles of the identical diameter a, whose surface potential was assumed to be 25 mV are shown. The particles were in a dispersion medium characterized by a Debye radius of $1 / \kappa = 10$ nm. Fig. 4 shows that the dependency $U(H)= U_d(H) + U_e(H)$ goes via a potential barrier, which is referred below as U_b. The magnitude of the potential barrier U_b for the largest particles $a = 1000$ nm, which can be referred to as regular colloid particles, is equal to 280 kT. The height of the barrier, U_b, decreases to 26 kT as the particle diameter decreases to 100 nm and decreases further to 4 kT for particle size of 20 nm.

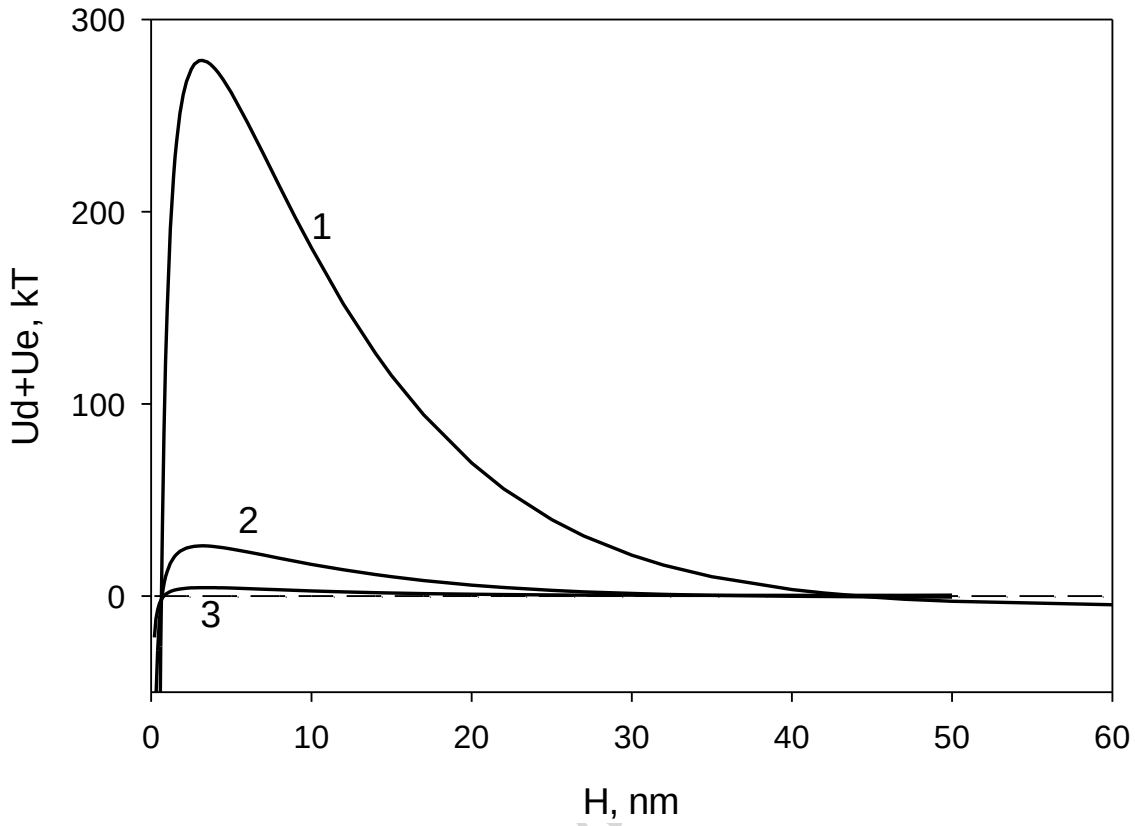

Figure 4. The results of calculations using Eqs. (3) and (5) depend on the sum of the energy of molecular attraction U_d and electrostatic repulsion U_e from the shortest distance H between the surfaces of two spherical particles with diameters 1) *a = 1000 nm;* 2) *a =100 nm;* and 3) *a = 20 nm*. Particle surface potential ψ*= 25 mV*, Debye radius *1 / k = 10 nm*.

The decrease in the Debye radius, $1/\kappa$, reduces the range of electrostatic forces and results in a smaller potential barrier, U_b. A decrease of the surface potential also results in the lowering of the potential barrier. For colloidal particles (a = 1000 nm) with lower surface potential, ψ=15 mV, the situation, as follows from Fig. 5, is even more interesting: when reducing the Debye radius down to $1/\kappa$ =3 nm the potential barrier disappears, and colloidal system loses stability.

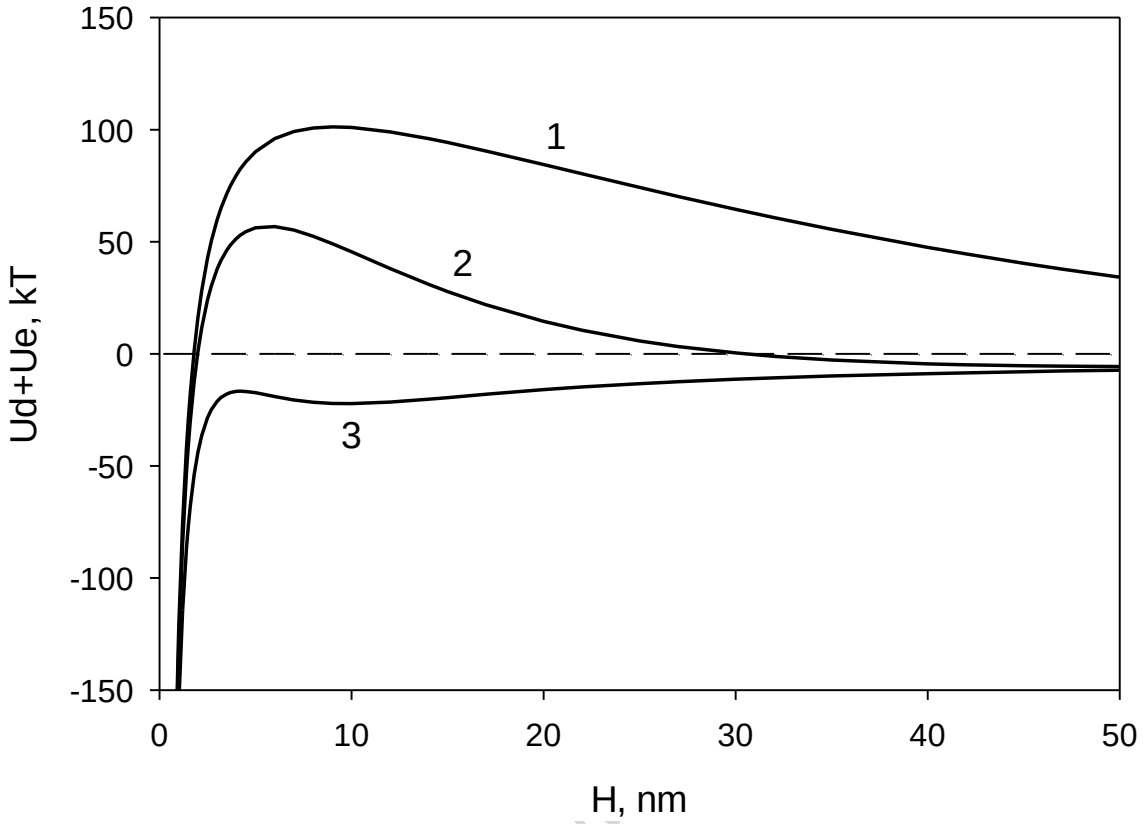

Fig. 5. The results of calculations of the total energy of interaction $U(H) = U_d(H) + U_e(H)$ for particles with diameter $a = 1000$ nm at a potential of the surface of the particles $\psi = 15$ mV and for three different values of Debye radius: 1) $1/\kappa$ = 30 nm; 2) 10 nm and 3) 3 nm.

The data presented in Figs. 4 and 5 showed that the height of the potential barrier U_b decreases linearly with a decrease of the particle size at constant surface potentials of small particles and the magnitudes of the Debye radius $1/\kappa$ that determines the long-range electrostatic forces. Therefore, a decrease of particle size should reduce the stability of the nano-dispersions. This suggests that nano-dispersions can be stable only with particle sizes above a certain critical value, depending on the physical properties of the particle material and the composition of the dispersion medium.

Thus, there may be some lower limit of particle sizes of stable nano-dispersions: the nano-dispersion becomes unstable if the particle size is below some critical radius a_{cr}. The critical radius, a_{cr}, decreases with the charge of the particles

and the increase of concentration of the electrolyte background solution. In general, stable nano-dispersions should not contain particle fractions with sizes smaller than the critical values.

In Fig. 6 calculated values of potential barriers, U_b, for particles of different radius are compared. As can be seen from this figure, the magnitude of the potential barrier, that determines the stability of the dispersion, increases linearly with increasing particle sizes. U_b values, at all other identical conditions, depend both on the potential of the particle surface ψ, and on the ionic strength of the dispersion medium, characterized by the value of the Debye radius $1/\kappa$. The comparison of the above data (Fig. 6) shows that a large height of the potential barrier can be achieved (at the identical value of the Hamaker constants) primarily by a high electric potential of the particle surface, ψ, and a low ionic strength of the dispersion medium corresponding to large Debye radii.

The stability of nano-dispersions is increasing (Fig. 6) in all cases with increasing particle size. To maintain high stability of nano-dispersions, it is necessary to provide a high electric charge of the particle surface and use dilute electrolyte solutions as a dispersion medium of nano-dispersion.

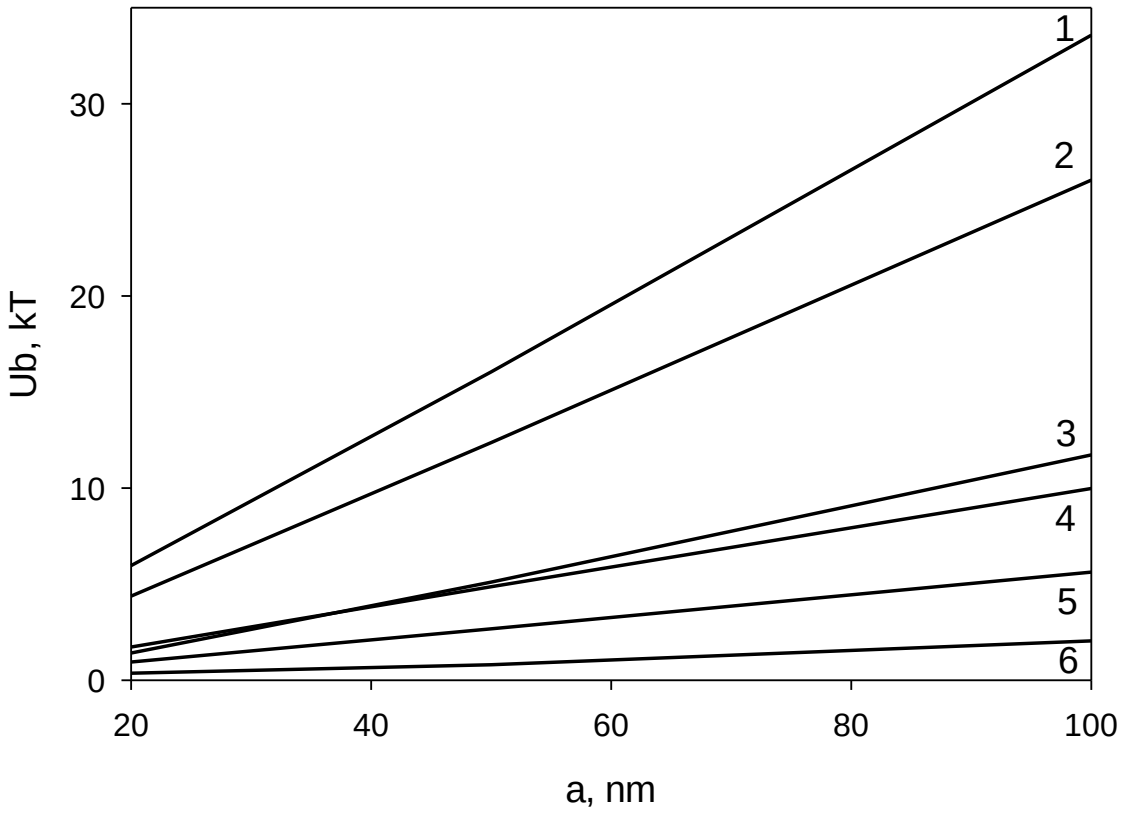

Fig. 6. The obtained dependences of the height of potential barriers U_b on the particle diameter *a* for various combinations of parameters, such as the particle surface potential and the Debye radius 1/κ: 1) ψ= 25 mV and 1 / κ = 30 nm; 2) ψ=25 mV and 1 / κ = 10 nm; 3) ψ= 25 mV and 1/κ = 3 nm; 4) ψ=15 mV and 1/κ= 30 nm; 5) ψ= 15 mV and 1 /κ =10 nm; 6) ψ= 10 mV and 1 /κ=30 nm.

Let us briefly discuss one extra component of nano-particle interaction, which was not discussed (for a very good reason) earlier: the structural component of interaction between nano-particles. The reason is that currently close to nothing is known from the theoretical point of view about this component in spite of considerable efforts invested.

In this part we prefer to deal with the so called Derjaguin's pressure (or disjoining/conjoining pressure) $\Pi(h)$. The interaction energy, *U*, is equal to the integral of the Derjaguin's pressure: $U = \int_h^\infty \Pi(h)dh$. In the case of structural component, the latter is caused by orientation of water molecules in a vicinity of nano-particle.

The water molecule can be modelled as an electric dipole. In a vicinity of a negatively charged interface in aqueous solution a positive part of water dipoles is attracted to the surface. That is, the negative part of dipole is directed oppositely, which in turn results in the orientation of the next layer of dipoles and so on. However, thermal fluctuations try to destroy this orientation.

Because of these two opposite trends a finite layer forms where the structure of water dipoles differs from the completely random bulk structure. This layer is frequently referred to as "a hydration layer". If now we have interfaces of two nano-particles with hydration layers close to each of them (or even one of them) then at a close separation, comparable with the thickness of the hydration layer, these surfaces "feel each other", that is, hydration layers overlap. The latter results either in attraction or repulsion of these nano-particle surfaces.

Unfortunately, up to now there is no firm theoretical background of the structural component of disjoining pressure even in the case of regular big colloidal particles. It is still impossible to deduce theoretically in which case the structure formation results in an attraction and in which case in a repulsion of particles or nano-particles. However, there is a semi-qualitative consideration of structural forces presented in [27], see also a review on the subject [28]. The total structural

component of Derjaguin's pressure in this case can be presented in the following form [29, 30]:

$$\Pi_S(h) = K_1 e^{-h/\lambda_1} + K_2 e^{-h/\lambda_2}, \qquad (9)$$

where K_1, K_2 and λ_1, λ_2 are parameters related to the magnitude and the characteristic length of the structural forces. The subscripts 1 and 2 correspond to the short-range and long-range structural interactions, respectively. Currently the latter four constants can be extracted from experimental data only.

There is a clear physical meaning of only one parameter $1/\lambda_1$, which is the correlation length of water molecules in aqueous solutions. The latter gives $1/\lambda_1 \sim 10\text{-}15$ $\mathring{A}$, which is the characteristic thickness of the hydration layer [1, 2].

Interest in structural forces has varied over a long period of time: an increase of interest followed by a decrease. This is due to the lack of an accurate theory of these forces. Churaev and Sobolev [31] attempted an estimation of the structural forces from available experimental data from the contact angle measurements. They put forward an assumption that the value of the constants in the equation for structural forces (9) depends on the potential of the surface of a solid.

If nanoparticles are coated by polymer and placed in a good solvent, additional steric repulsive force comes into play when the polymer chains begin to overlap. This force is the result of entropy decrease due to decrease of volume available to each chain. Using the de Gennes' equation [32] for interaction between 2 plates covered by polymers (high surface coverage) and Derjaguin's approximation, the following expression for the interaction potential due steric repulsion between two spherical particles was found in [33].

$$U_{ST}(H) = \frac{64\pi a L^2}{s^3} kT \left\{ \frac{1}{5}\left(\frac{H}{2L}\right)^{-1/4} - \frac{1}{77}\left(\frac{H}{2L}\right)^{\frac{11}{4}} + \frac{3}{35}\left(\frac{H}{2L}\right) - \frac{3}{11} \right\}, \qquad (10)$$

where H is the surface to surface distance between particle cores, L is the thickness of the polymer layer and s is the average distance between the chain attachment points. Israelachvili [8] proposed a simplified expression

$$U_{ST}(H) = \frac{100L}{\pi s^3} kT e^{-\pi H/L} \qquad (11)$$

valid for $0.2 < H/2L < 0.9$.

Eqs. (10) and (11) were derived using Derjaguin's approximation, therefore they valid only when the core size is considerably larger than the thickness of polymer

layer. For small nanoparticles only several polymer chains can get into the contact zone, moreover they can deform and move from the gap between the particles. Therefore Eqs. (10) and (11) will overestimate steric interactions for small nanoparticles. There is no generally accepted theory for particle interaction under condition $a \leq L$.

There is a huge amount of literature on numerical simulations of interactions between nanoparticles including various algorithms such as Monte Carlo, molecular dynamics, density functional theory etc. This literature needs separate comprehensive discussion and therefore is not addressed here. Some simulation results are discussed for example in [7]

3. Experimental techniques for measurement of nanoparticle interactions.

There are a number of techniques which can directly measure the interaction forces between individual colloidal particles, including, but not exclusively, atomic force microscopy (AFM) [34], total internal reflectance microscopy [35], optical tweezers [36], electrophoresis [37] etc. However, for various reasons many of these techniques are not suitable or have not been adopted for measurements using particles in the nano-size range. In this section we briefly discuss two techniques which are capable of such measurements.

3.1. Atomic Force Microscopy

In addition to its original application for high resolution imaging, the technique of AFM has been used extensively for the measurement of long range and adhesion forces between many materials under a wide range of conditions [34, 38, 39]. Whilst many of these works have focussed on functionalised probes versus flat surfaces or by using particles of micrometre size, measurements using nanoparticles positioned at the end of probe tips are also possible.

In essence the AFM consists of a sharpened probe mounted close to the end of a flexible microcantilever. As this cantilever behaves as a simple spring with a linear force versus deflection response within typical operating parameters, monitoring the deflection of the lever can serve as a direct measure of the forces acting upon the probe tip. Depending upon the configuration of the particular instrument, either the sample or the chip hosting the cantilever – probe assembly are mounted upon a piezo crystal, which allows relative motion of the tip and sample in all spatial

directions, allowing scanning into and out of contact with the sample in addition to lateral scanning.

Cantilever deflection is most commonly measured by use of an optical lever system, whereby a laser is reflected from the reverse side of the cantilever onto a position sensitive photodetector. By the appropriate calibration steps to characterise both the mechanical compliance of the cantilever arm and the response of the optical lever system, deflection of the lever can be converted from a raw signal (typically recorded in nA or V) to deflection in nm and finally to force in N. By subtracting the deflection distance from the travel distance of the piezo in the *z* – direction distance moved by the probe tip can be obtained. The final step is to assign a zero-distance point, which then allows a plot of interaction force versus tip displacement to be made. The assignment of a point of zero separation distance, in all but the most simple of cases, is non-trivial, especially in the case of adsorbed thin films and deformable surfaces or interfaces. The basic operation and calibration processes are covered elsewhere in more detail [38, 40].

An example force versus separation distance curve from a particle-surface interaction is shown in Fig. 7. Here repulsive forces are set as positive. At large separation distances no net interaction forces are detected. As close approach is made, repulsive interaction forces (positive values on the chart) are detected, followed by a linear repulsive force after hard contact is made. As the probe is retracted from the surface a hysteresis is observed, with attractive forces observed before the probe disengages from the surface, due to adhesion, before returning to no net force as the probe snaps from the surface.

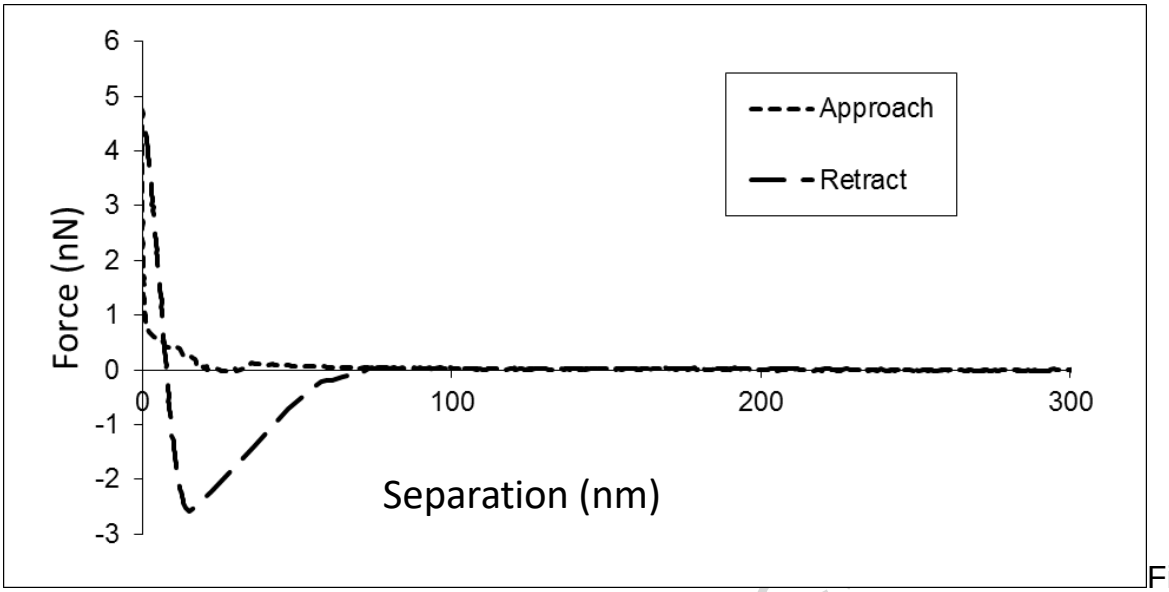

Fig. 7. Example force/distance curve from AFM measurements.

In most AFM force measurements, the imaging probe is either chemically functionalised or replaced entirely with a particle of colloidal size (typically ~3-15 μm diameter), either itself functionalised or composed of a material of interest. For this latter approach particles are attached to the apex of a tipless microcantilever using either a micromanipulator or AFM instrument stage whilst observing using an optical microscope set-up. As such, for nanoparticle measurements this arrangement is not suitable, so other methods need to be employed. Several researchers have examined other approaches to affixing nanoparticles to AFM probes for direct nanoparticle force measurements.

Ong and Sokolov [41] coated the imaging tip of an AFM with a thin layer of epoxy resin, which they dipped into a powder of ceria nanoparticles when the epoxy was almost set. This resulted in a cluster of nanoparticles on the probe tip. Imaging of the tip using a sharp calibration standard confirmed that the clusters in all cases were terminated by single nanoparticles, allowing single nanoparticle measurements with SiO_2 surfaces to be made in aqueous solution at different pH values. Whilst the results for nanoparticles were qualitatively different compared with larger particles, the authors attributed this to different preparation methods for the two types of particles, rather than inherent differences due to size alone.

A wet chemistry approach was used by Vakarelski and Higashitani [42] to append single 10-40 nm diameter gold nanospheres to the apex of AFM probes. Firstly, the probes were coated with a passivation layer, which was then selectively removed

from the imaging tip apex by scanning across a silicon wafer. This allowed the apex to be selectively functionalised, allowing gold nanoparticles to be specifically attached at this point. Fitting of DLVO theory to force distance curves showed an apparent change in Debye length with particle size, and deviations of forces scaled for particle size, which were attributed to the invalidity of the Derjaguin approximation for small particle sizes. Previously, gold nano-particle terminated tips had also been produced by direct growth of nanoparticles on AFM probes, rather than by attachment [43].

Salameh et al combined AFM force measurements with molecular dynamics simulations to investigate forces between nanoparticles in nanomaterials [44]. An aggregate film of TiO2 nanoparticles was repeatedly perturbed by an AFM probe under ambient conditions and interaction force curves were examined for multiple events in the retraction part of the force curves, caused by sliding, rolling and detachment of particles. For this system particle interaction forces were found to be dominated by layers of adsorbed water, generating a characteristic particle detachment force of 2.5 nN.

Whilst the measurement of interaction forces between particles in the micron range has been repeated many times with various materials, measurements using individual nanoparticles is not as well described. One major issue is that if the nanoparticles in question have diameters smaller than the range of surface forces then some of the measured interaction forces may of necessity be due to interactions between the substrates they are adsorbed to. Whilst this is not a problem when measurements are between multiple particles, for single particle measurements this is a difficult problem, and a possible reason why these measurements are not more often found in the literature.

3.2. Electrophoresis

Electrophoretic techniques are a well-established method for the determination of zeta potentials of dispersed colloidal particles. Electrophoresis consists of a static aqueous phase, with dispersed particles moved by an applied electrical field. Due to the simplicity of the approach and relatively easy data collection, this is the primary method for particle zeta potential measurement. The measurement chamber contains oppositely charged electrodes and is then filled with an electrolyte solution of a particular pH, ionic strength and composition, with the particles of interest

dispersed. Particles will migrate towards the oppositely charged electrodes with an electrophoretic mobility, U_E, related to the equilibrium velocity, which can be used to calculate the zeta potential from Henry's equation:

$$U_E = {}^{2}/_{3} \frac{\varepsilon_0 \varepsilon_r \psi}{\eta} f(\kappa a) \quad (12)$$

where η is the electrolyte viscosity, ψ is the particle zeta-potential as before, f(κa) is Henry's function [13], where 1/κ is the Debye radius and *a* particle radius. In the case of small particles and weak electrolyte the Hückel approximation can be applied, where f(κa) =1 [13]:

$$\psi = {}^{3}/_{2} \frac{U_E \eta}{\varepsilon_o \varepsilon_r}. \quad (13)$$

The latter approximation is most suitable for nanoparticles, where the particle radius is smaller the Debye length.

3.2.1. Differential electrophoresis

A technique based upon electrophoresis has been developed, called differential electrophoresis, for the measurement of the interaction forces between two colloidal particles [45]. The technique centres around the balance of colloidal forces between two different particles holding them together and the different forces applied by an electric field when those two particles have different surface potentials. As the applied electrical field is increased the two-particle doublet will go from rotating in that field to be aligned with it, with a displacement force acting against the colloidal interaction, and sundering it at a suitably high value [46]. The force acting on the doublet when aligned with the electric field is given by [37]:

$$F_{disp} = 3\pi a_2 \varepsilon_0 \varepsilon_r \left[\psi_1 - \psi_2\right] E\, Q \quad (14)$$

where F_{disp} is the displacement force applied by the electric field, E, a_2 is the radius for the larger of two particles, and Q is a dimensionless coefficient, which incorporates the ratios of sizes of the two interacting particles. At large separations Q is equal to 2β/(1+β), where β is the ratio of small to large particles. It is worth noting that zeta potential applies to the electric potential at the no-slip boundary between tightly bound ions to the particle surface, rather than the actual particle surface. As such, the relevant radius (i.e from the centre to the no-slip boundary) may differ from the actual particle radius without bound ions.

From monitoring through a microscope the point at which the two particles disengage, the force at which the colloidal interaction force is equal to the

displacement force can be ascertained. This adaptation of electrophoresis is capable of performing force measurements between individual nanoparticles. Velegol et al [47] succeeded in making measurements between polystyrene spheres as small as 85 nm in diameter. Forces measured varied between 0.1 to 10 pN, which was in reasonable agreement with the values expected from theoretical calculations.

4. Experimental studies of nano-particle interactions

Extensive experimental study on behaviour and aggregation properties of nano-dispersion was motivated by growing areas of their application as well as by ecological problems caused by subsequently growing release of manufactured nanoparticles into environment [48, 49].

A separate branch of nano-particle study is their interactions and self-assembly on liquid/liquid and liquid/air interface, where DLVO forces can be modified and new forces, such as capillarity or thermal fluctuations come into play [50, 51]. Adsorption of nano-particles at the interface is broadly used for stabilisation of foams [52] and emulsions [53]. Tailored self-assembly of nanoparticles at the interface with possibility their further transfer onto solid surface also open wide perspectives in development of new materials [51, 54].

Typical nanoparticles include not only solids, such as metal, oxides, etc., but also soft particles, such as self-assembled structures, micelles, vesicles, bilayers, as well as polymers and proteins. The latter have complicated structure and charge distribution over the nano-particle surface. Soft nano-particles can be further functionalised by using core-shell structure and are of great interest nowadays due to its use in drug delivery, bioseparation etc. [55, 56].

Non-organic nanoparticles also can poses the core-shell structure by coating with other metals or polymers for additional stabilisation/functionality to use , for example, in drug delivery [57], imaging techniques [58], medicine [59] etc. Overall, the effects of surface topology and non-uniform charge distribution becomes very important on the nanometre length scale. Here we consider experimental results on solid non-organic nano-particles, for which the main interaction forces are dispersion, electrostatic and structural forces discussed above.

The measurement of zeta-potential even for solid nanoparticles is not straightforward. The commercially available instruments usually use the

Smoluchowski approximation to calculate zeta-potential of aqueous suspensions from the measured electrophoretic velocity. This approximation is valid for the case $\kappa a >> 1$ which is often not satisfied for nanoparticles. Therefore when the size of particles decreases and becomes of the same order of magnitude or smaller than Debye radius, the values of zeta-potential should be corrected. This correction should take into account a non-uniform distribution of electrolyte induced by the electric current in the liquid surrounding the nano-particle. The respective procedure is discussed in detail in [60]. The complexity of measurement of zeta-potential for metallic nanoparticles is addressed in [61].

For metal oxide, e.g. TiO_2, nanoparticles a decrease of size results in the shift of the point of zero charge (PZC) to higher pH values [62], whereas surface charge density increases [63]. Similar results were obtained also in numerical simulations [64, 65]. The effect is most pronounced for the particle size below 10 nm, when the nanoparticle curvature becomes comparable with the curvature of hydrated ions. According to [65] the surface charge starts decreasing significantly when the ratio of electrical double layer thickness to the particle diameter becomes larger than 0.2. At the same time the shift of PZC to the higher pH values with an increase of the size was observed in [66] for SiO_2 nanoparticles in the size range 9 – 113 nm, whereas in [67] the observed shift of PZC to the lower pH values with an increase in particles size was ascribed to the larger amount of impurities, such as SiO_2, in the larger particles. All reported values of PZC are in the range reported in the literature [68, 69] for macroscopic systems. Therefore, the size dependence is not conclusive and could be due to different surface chemistry of particles related to their synthesis.

For small nanoparticles, zeta-potential depends also on the particle's volume fraction, even at very small volume fractions, due to interaction of electrical double layers. For example, a monotonous decrease in zeta-potential was reported for maghemite nanoparticles of 6 nm in the range of volume fractions 0.1 – 5 % [70].

Stability of nano-dispersions depends considerably on the particles shape. Suspension formed by spheres is more stable than the suspension formed by the rods of the same diameter [71].

For relatively large solid nanoparticles (a > 10 nm) usually there is a reasonable qualitative agreement with predictions based on DLVO theory. For example, decrease in critical coagulation concentration (CCC) of electrolyte (NaCl) with decrease of particles size was observed experimentally in [72] by study of

aggregation of uncoated hematite nanoparticle with diameters 24, 64 and 130 nm. Calculations performed in [72] according to DLVO theory using experimentally measured values of zeta-potential have shown decrease of potential barrier with decrease of particle size. Similar results were obtained for TiO2 nanoparticles in [67]. These results agree with theoretical predictions discussed earlier.

In [73] stability of dispersions of non-coated angular silica particles of effective diameter 25 nm was studied in the range of pH and in presence of various salts: NaCl, $CaCl_2$, $BaCl_2$, and $MgCl_2$. The high stability of silica against coagulation was confirmed in [74], in particular, it was observed that nano-dispersions of silica are stable even in proximity of the isoelectric point, where the surface charge is close to zero. Therefore, an additional mechanism of stabilization, besides the electrostatic one should be in action for silica nanoparticles, such as for example a shift of surface charges location to outside the solid/liquid interface and/or a steric repulsion of flexible protruding surface groups [74]. It was found that addition of electrolyte destabilizes silica nano-suspensions and CCC for monovalent salt (NaCl) was two orders of magnitude higher than that for divalent salts in good agreement with the Shulze–Hardy rule [75]. For the divalent salts however, ion-specific effect was observed: $MgCl_2$ has two times smaller CCC than $CaCl_2$ and $BaCl_2$. Note, ion-specific effects are out of scope of DLVO theory.

In [76] for dispersion of bare CeO_2 nanoparticles with radii in the range 5-20 nm existence of stable small irreversibly aggregated clusters with hydrodynamic radius ~ 37 nm were found. Aggregation of these clusters was studied in the presence of NaCl and $CaCl_2$. Good agreement with DLVO theory was found for dispersions containing NaCl. The value of CCC for two-valent $CaCl_2$ was five times smaller as compared with mono-valent NaCl. This difference is smaller than expected according to the Shulze–Hardy rule $\sim Z^6$, which is ascribed in [76] to cation adsorption to the surfaces of nanoparticles, where Z is the counterion valency.

For coated nanoparticles specific ion effects become even more pronounced. According to [77], for gold nanoparticles coated with polymers CCC in NaCl solution was noticeably higher than that in KCl solution. Moreover, in complete qualitative contradiction to Shultz–Hardy rule CCC for divalent electrolytes, $MgCl_2$ and $SrCl_2$, was higher than for monovalent electrolytes. In fact, CCC values found in [77] followed the Hofmeister series.

Effect of environmental parameters on stability of nanoparticles is reviewed in [75] and effect of particles functionalisation is reviewed in [78].

5. Conclusions

The authors have not attempted to cover all available literature in the area but instead have tried to underline the fundamental problems in the area which need to be understood.

An important feature of interactions between nanoparticles is that the range of surface forces action is larger than the nano-particle's radius. To the best of the authors knowledge, there is no complete theory for these interactions. As a result of a large radius of interaction relative to the particle size, the critical volume concentration of nano-suspensions (the concentration when all particles interact) is very low in comparison with colloidal suspension of micron size particles.

At concentrations above critical the interaction between nanoparticles cannot be treated as pairwise but becomes a collective one. To the best of the author's knowledge, there is not a single attempt to take this into account.

The diffusion coefficient of nanoparticles is substantially greater than the corresponding coefficient of regular colloidal particles.

The physical nature of interactions between nanoparticles is the same as that between the regular colloidal particles. However, the large radius of interaction relative to the particle size makes it possible currently to only investigate pairwise interactions, which has to be adjusted to the main feature of nanoparticles: vdW interactions should include some extra term and zeta-potential remains a very important property of nanoparticles. However, measurement of zeta-potential of nanoparticles requires a more sophisticated approach than for regular colloidal particles. Structural interactions between nanoparticles is still yet to be understood.

Experimental results for interactions in suspensions of bare nano-particles are in a good qualitative agreement with modified DLVO theory. However strong ion-specific effects have been observed in many experimental studies. Ion-specific effects are more pronounced for coated nano-particles.

Acknowledgement

Nina Kovalchuk acknowledges the EPSRC Programme Grant MEMPHIS (EP/K003976/1); Daniel Johnson and Nidal Hilal would like to acknowledge the Royal Society for funding their contribution to this work through a Royal Society International Collaboration Award (IC160133); Vladimir Sobolev acknowledges support from Russian Fund for Basic Research (RFBI); Victor Starov's research was supported by CoWet Marie Curie EU grant, PASTA and MAP EVAPORATION projects, European Space Agency.

References

1. Liang, Y., et al., *Interaction forces between colloidal particles in liquid: theory and experiment.* Adv Colloid Interface Sci, 2007. **134-135**: p. 151-66.
2. *Nanoscience. Colloidal and Interfacial Aspects*. Surfactant Science Series, ed. V. Starov. 2010: CRC press Taylor & Frances Group. 1216.
3. Mahbubul, I.M., R. Saidur, and M.A. Amalina, *Latest developments on the viscosity of nanofluids.* International Journal of Heat and Mass Transfer, 2012. **55**(4): p. 874-885.
4. Koca, H.D., et al., *Effect of particle size on the viscosity of nanofluids: A review.* Renewable and Sustainable Energy Reviews, 2018. **82**: p. 1664-1674.
5. Khodadadi, H., et al., *A comprehensive review on rheological behavior of mono and hybrid nanofluids: Effective parameters and predictive correlations.* International Journal of Heat and Mass Transfer, 2018. **127**: p. 997-1012.
6. Derjaguin, B.V., N.V. Churaev, and V.M. Muller, *Surface Forces*. 1987, New York: Consultants Bureau.
7. Batista, C.A., R.G. Larson, and N.A. Kotov, *Nonadditivity of nanoparticle interactions.* Science, 2015. **350**(6257): p. 1242477.
8. Israelachvili, J.N., *Intermolecular and surface forces*. 2nd ed. 1992, Boston: Academic Press.
9. Derjaguin, B.V., Zh. Phys. Chem. (in Russian), 1935. **6**: p. 1306-1319.
10. Bowen, W.R., et al., *A model of the interaction between acharged particle and a pore in a charged membrane surface.* Adv Colloid Interface Sci, 1999. **81**: p. 35-72.
11. Derjaguin, B.V., News of AoS the USSR, Chemistry, 1937. **5**.
12. McCartney, L.N. and S. Levine, *An improvement on Derjaguin's expression at small potentials for the double layer interaction energy of two spherical colloidal particles.* J Colloid Interface Sci, 1969. **30**: p. 345-354.
13. Hunter, R.J., *Foundation of Colloid Science*. 2nd ed. 2001, Oxford: Oxford University Press.
14. Kostoglou, M. and A.J. Karabelas, *The effect of discrete surface charge on potential energy of repulsion between colloidal surfaces.* J Colloid Interface Sci, 1992. **151**: p. 534-545.
15. Velegol, D. and P.K. Thwar, *Analytical Model for the Effect of Surface Charge Nonuniformity on Colloidal Interactions.* Langmuir, 2001. **17**: p. 7687-7693.
16. Stenhammar, J. and M. Trulsson, *Classical van der Waals interactions between spherical bodies of dipolar fluid.* Phys Rev E Stat Nonlin Soft Matter Phys, 2011. **84**(1 Pt 1): p. 011117.
17. Kirsch, V.A., *Calculation of the van der Waals force between a spherical particle and an infinite cylinder.* Advances in Colloid and Interface Science, 2003. **104**(1-3): p. 311-324.
18. Yannopapas, V., *Fluctuational-Electrodynamics Calculations of the van der Waals Potential in Nanoparticle Superlattices.* The Journal of Physical Chemistry C, 2013. **117**(29): p. 15342-15346.
19. van Kampen, N.G., B.R.A. Nijboer, and K. Schram, *On the macrscopic theory of van der Waals forces.* Physics Letters, 1968. **26A**: p. 307-308.

20. Casimir, H.B.G. and D. Polder, *The Influence of Retardation on the London-van der Waals Forces.* Physical Review, 1948. **73**(4): p. 360-372.
21. Barash, J.S. and V.L. Ginzburg, JETP Letters (in Russian), 1972. **15**.
22. Mitchell, D.J. and B.W. Ninham, *van der Waals Forces between Two Spheres.* The Journal of Chemical Physics, 1972. **56**(3): p. 1117-1126.
23. Fernandez-Varea, J.M. and R. Garcia-Molina, *Hamaker Constants of Systems Involving Water Obtained from a Dielectric Function That Fulfills the f Sum Rule.* J Colloid Interface Sci, 2000. **231**(2): p. 394-397.
24. Jiang, K. and P. Pinchuk, *Temperature and size-dependent Hamaker constants for metal nanoparticles.* Nanotechnology, 2016. **27**(34): p. 345710.
25. Krupp, H., *Particle adhesion. Theory and experiment.* Adv Colloid Interface Sci, 1967. **1**: p. 111-239.
26. Rabinovich, Y.I. and N. Churaev, Colloid. Journal (in Russian), 1975. **41**.
27. Djikaev, Y.S. and E. Ruckenstein, *The variation of the number of hydrogen bonds per water molecule in the vicinity of a hydrophobic surface and its effect on hydrophobic interactions.* Current Opinion in Colloid & Interface Science, 2011. **16**(4): p. 272-284.
28. Donaldson, S.H., Jr., et al., *Developing a general interaction potential for hydrophobic and hydrophilic interactions.* Langmuir, 2015. **31**(7): p. 2051-64.
29. Kuchin, I. and V. Starov, *Hysteresis of Contact Angle of Sessile Droplets on Smooth Homogeneous Solid Substrates via Disjoining/Conjoining Pressure.* Langmuir, 2015. **31**(19): p. 5345-52.
30. Arjmandi-Tash, O., et al., *Kinetics of Wetting and Spreading of Droplets over Various Substrates.* Langmuir, 2017. **33**(18): p. 4367-4385.
31. Churaev, N.V. and V.D. Sobolev, *Contribution of structural forces to wetting of quartz surface by electrolyte solutions.* Colloid Journal, 2000. **62**: p. 244-250.
32. de Gennes, P.G., *Polymers at an interface; a simplified view.* Adv Colloid Interface Sci, 1987. **27**: p. 189-209.
33. Berli, C.L.A. and D. Quemada, *Prediction of the Interaction Potential of Microgel Particles from Rheometric Data. Comparison with Different Models.* Langmuir, 2000. **16**(26): p. 10509-10514.
34. Ducker, W.A., T.J. Senden, and R.M. Pashley, *Direct measurement of colloidal forces using an atomic force microscope.* Nature, 1991. **353**(6341): p. 239.
35. Bevan, M.A. and D.C. Prieve, *Direct measurement of retarded van der Waals attraction.* Langmuir, 1999. **15**(23): p. 7925-7936.
36. Grier, D.G., *A revolution in optical manipulation.* Nature, 2003. **424**(6950): p. 810.
37. Thwar, P.K. and D. Velegol, *Force measurements between weakly attractive polystyrene particles.* Langmuir, 2002. **18**(20): p. 7328-7333.
38. Butt, H.-J., B. Cappella, and M. Kappl, *Force measurements with the atomic force microscope: Technique, interpretation and applications.* Surface Science Reports, 2005. **59**(1): p. 1-152.
39. Hilal, N., et al., *Measurement of particle and surface interactions using force microscopy.* Atomic Force Microscopy in Process Engineering. Butterworth-Heinemann, Oxford, 2009: p. 31-80.
40. Johnson, D., N. Hilal, and W.R. Bowen, *Basic principles of atomic force microscopy*, in *Atomic force microscopy in process engineering: An introduction to AFM for improved processes and product, UK, IChemE*. 2009.
41. Ong, Q.K. and I. Sokolov, *Attachment of nanoparticles to the AFM tips for direct measurements of interaction between a single nanoparticle and surfaces.* Journal of Colloid and Interface Science, 2007. **310**(2): p. 385-390.
42. Vakarelski, I.U. and K. Higashitani, *Single-nanoparticle-terminated tips for scanning probe microscopy.* Langmuir, 2006. **22**(7): p. 2931-2934.

43. Barsegova, I., et al., *Controlled fabrication of silver or gold nanoparticle near-field optical atomic force probes: Enhancement of second-harmonic generation.* Applied Physics Letters, 2002. **81**(18): p. 3461-3463.
44. Salameh, S., et al., *Adhesion mechanisms of the contact interface of TiO2 nanoparticles in films and aggregates.* Langmuir, 2012. **28**(31): p. 11457-11464.
45. Velegol, D., J.L. Anderson, and S. Garoff, *Determining the forces between polystyrene latex spheres using differential electrophoresis.* Langmuir, 1996. **12**(17): p. 4103-4110.
46. Anderson, J.L., D. Velegol, and S. Garoff, *Measuring colloidal forces using differential electrophoresis.* Langmuir, 2000. **16**(7): p. 3372-3384.
47. Velegol, D., et al., *Force measurements between sub-100 nm colloidal particles.* Langmuir, 2007. **23**(3): p. 1275-1280.
48. Canesi, L. and I. Corsi, *Effects of nanomaterials on marine invertebrates.* Sci Total Environ, 2016. **565**: p. 933-940.
49. Bundschuh, M., et al., *Nanoparticles in the environment: where do we come from, where do we go to?* Environ Sci Eur, 2018. **30**(1): p. 6.
50. Binks, B.P., *Particles as surfactantssimilarities and differences.* Current Opinion in Colloid & Interface Science, 2002. **7**: p. 21-41.
51. Bresme, F. and M. Oettel, *Nanoparticles at fluid interfaces.* J Phys Condens Matter, 2007. **19**(41): p. 413101.
52. Stocco, A., et al., *Aqueous foams stabilized solely by particles.* Soft Matter, 2011. **7**(4).
53. Marina, P.F., et al., *Van der Waals Emulsions: Emulsions Stabilized by Surface-Inactive, Hydrophilic Particles via van der Waals Attraction.* Angew Chem Int Ed Engl, 2018. **57**(30): p. 9510-9514.
54. Maestro, A., *Tailoring the interfacial assembly of colloidal particles by engineering the mechanical properties of the interface.* Current Opinion in Colloid & Interface Science, 2019. **39**: p. 232-250.
55. Eslami, P., F. Rossi, and S. Fedeli, *Hybrid Nanogels: Stealth and Biocompatible Structures for Drug Delivery Applications.* Pharmaceutics, 2019. **11**(2).
56. Panday, R., et al., *Amphiphilic core-shell nanoparticles: Synthesis, biophysical properties, and applications.* Colloids Surf B Biointerfaces, 2018. **172**: p. 68-81.
57. Silva, J.Y.R., et al., *A thermo-responsive adsorbent-heater-thermometer nanomaterial for controlled drug release: (ZIF-8,EuxTby)@AuNP core-shell.* Mater Sci Eng C Mater Biol Appl, 2019. **102**: p. 578-588.
58. Silvestri, B., et al., *Silver-nanoparticles as plasmon-resonant enhancers for eumelanin's photoacoustic signal in a self-structured hybrid nanoprobe.* Mater Sci Eng C Mater Biol Appl, 2019. **102**: p. 788-797.
59. Wilczewska, A.Z., et al., *Magnetic nanoparticles bearing metallocarbonyl moiety as antibacterial and antifungal agents.* Applied Surface Science, 2019. **487**: p. 601-609.
60. Felix, C., et al., *Electrophoresis and stability of nano-colloids: history, theory and experimental examples.* Adv Colloid Interface Sci, 2014. **211**: p. 77-92.
61. Skoglund, S., et al., *Difficulties and flaws in performing accurate determinations of zeta potentials of metal nanoparticles in complex solutions-Four case studies.* PLoS One, 2017. **12**(7): p. e0181735.
62. Zhou, D., et al., *Influence of material properties on TiO2 nanoparticle agglomeration.* PLoS One, 2013. **8**(11): p. e81239.
63. Shi, Y.-R., et al., *Experimental Determination of Particle Size-Dependent Surface Charge Density for Silica Nanospheres.* The Journal of Physical Chemistry C, 2018. **122**(41): p. 23764-23771.
64. Abbas, Z., et al., *Size-Dependent Surface Charging of Nanoparticles.* J Phys Chem, 2008. **112**: p. 5715-5723.

65. Barisik, M., et al., *Size Dependent Surface Charge Properties of Silica Nanoparticles.* The Journal of Physical Chemistry C, 2014. **118**(4): p. 1836-1842.
66. Seo, J., et al., *Size-dependent interactions of silica nanoparticles with a flat silica surface.* J Colloid Interface Sci, 2016. **483**: p. 177-184.
67. Liu, X., G. Chen, and C. Su, *Effects of material properties on sedimentation and aggregation of titanium dioxide nanoparticles of anatase and rutile in the aqueous phase.* J Colloid Interface Sci, 2011. **363**(1): p. 84-91.
68. Kosmulski, M., *The pH-dependent surface charging and the points of zero charge.* J Colloid Interface Sci, 2002. **253**(1): p. 77-87.
69. Kosmulski, M., *The pH dependent surface charging and points of zero charge. VII. Update.* Adv Colloid Interface Sci, 2018. **251**: p. 115-138.
70. Lucas, I.T., et al., *Influence of the volume fraction on the electrokinetic properties of maghemite nanoparticles in suspension.* Molecular Physics, 2014. **112**(9-10): p. 1463-1471.
71. Degabriel, T., et al., *Factors impacting the aggregation/agglomeration and photocatalytic activity of highly crystalline spheroid- and rod-shaped TiO2 nanoparticles in aqueous solutions.* Phys Chem Chem Phys, 2018. **20**(18): p. 12898-12907.
72. He, Y.T., J. Wan, and T. Tokunaga, *Kinetic stability of hematite nanoparticles: the effect of particle sizes.* Journal of Nanoparticle Research, 2008. **10**(2): p. 321-332.
73. Metin, C.O., et al., *Stability of aqueous silica nanoparticle dispersions.* Journal of Nanoparticle Research, 2011. **13**(2): p. 839-850.
74. lsraelachvili, J. and H. Wennerstrom, *Role of hydration and water structure in biological and colloidal interactions.* Nature, 1996. **379**: p. 219-225.
75. Baalousha, M., *Effect of nanomaterial and media physicochemical properties on nanomaterial aggregation kinetics.* NanoImpact, 2017. **6**: p. 55-68.
76. Buettner, K.M., C.I. Rinciog, and S.E. Mylon, *Aggregation kinetics of cerium oxide nanoparticles in monovalent and divalent electrolytes.* Colloids and Surfaces A: Physicochemical and Engineering Aspects, 2010. **366**(1-3): p. 74-79.
77. Gambinossi, F., et al., *Aggregation kinetics of stimulus-responsive polymer-coated gold nanoparticles driven by Hofmeister effects.* Colloids and Interface Science Communications, 2015. **9**: p. 9-11.
78. Gambinossi, F., S.E. Mylon, and J.K. Ferri, *Aggregation kinetics and colloidal stability of functionalized nanoparticles.* Adv Colloid Interface Sci, 2015. **222**: p. 332-49.

Highlights

Interaction between nanoparticles
Multi-particles interactions
Experimental techniques
Experimental studies of nanoparticle interactions

Conflict of interests
Non conflict of interests